Scientia Iranica B (2013) 20(5), 1538–1549

SCIENTIA IRANICA

Sharif University of Technology
Scientia Iranica
Transactions B: Mechanical Engineering
www.scientiairanica.com

Evaluation of the modified 3D free-surface Green's function for potential flow in a numerical towing tank

A. Abbasnia and M. Ghiasi*

Department of Marine Engineering, Amirkabir University of Technology, Tehran, Iran.

Received 31 May 2012; received in revised form 23 December 2012; accepted 25 June 2013

KEYWORDS
The source;
Boundary-value problems;
Numerical towing tank;
Green's function;
Image method.

Abstract. What is derived in this paper is the potential flow around the marine structures in the numerical towing tank. The Green's formula and image method is employed to solve the boundary value problem. The Green's function satisfies the Laplace equation and the boundary conditions on the bottom, walls and free surface. The Green's function consists of three parts. The first part is correlated with spatial spacing between the source and a field point. The second part consists of the free surface disturbance. The radiation condition is dealt with in the third part to ensure that the waves vanish upstream of the source. An infinite series is obtained for each part of the Green's function using the image method. Effects of the numerical towing tank's width and depth on the solution are investigated, and the flow patterns due to the presence of a singularity with constant strength in the uniform flow are computed. Uniform motion of a submerged sphere and ellipsoid are simulated and compared with the analytical solutions and other numerical results. Wave profiles are computed for a sphere and an ellipsoid to show the effect of the tank width on the solution.

1. Introduction

Hydrodynamic analysis of the marine structures in the towing tanks is necessary for obtaining the perfect design in ocean engineering. The towing tanks have been widely used for various marine purposes one of which is to determine the performance of the marine structures in a uniform motion and the properties of flow around the body of the structure. Motions of structures in a harbor and the model test in the towing tank could be affected by side walls and the bottom (sea bed). Development of the Numerical Towing Tank (NTT) can help to account for the finite boundary effects induced by the walls and bottoms of the physical tanks and to make the test results more precise, which would eventually reduce the test cost.

*. *Corresponding author. Tel.: +98-21-66419615*
E-mail addresses: a_abbasnia@aut.ac.ir (A. Abbasnia), mghiasi@aut.ac.ir (M. Ghiasi)

The potential theory in computational hydrodynamics is widely used to characterize the interactions of fluid-marine structures. The governing equation in incompressible, inviscid fluid and irrotational flow is Laplace's equation whose solutions must satisfy the various boundary conditions. NTT boundary conditions consist of the free-surface boundary condition, the impermeable boundary conditions of the body, wall sides and the bottom, the inflow boundary condition and the radiation boundary condition of the outflow surface, to ensure that the waves vanish upstream of the disturbance. The Boundary Elements Method (BEM), based on the second Green's identity, has been employed to solve the boundary value problems with complex geometry of boundaries. The fundamental Green's function for a towing tank can be assumed to be the Green's function of a source with constant strength on the NTT where the boundary conditions are the conditions on the bottom, walls and the free surface. The fundamental Green's function can be used

with the body boundary condition for simulation of the flow on the NTT with presence of the body. Other boundary conditions are satisfied spontaneously.

Various Green's functions were presented in complex and algebraic formulations for two and three dimensional problems by Wehausen & Laitone [1]. The Green's function is approximated by solving the place-Laplace equation in different computational domains and specified boundary conditions. The approximation algorithm of the fundamental solution has been based on Fourier transforms space and inverse Fourier transforms given by Newman [2]. Evaluation of a Principal Value (PV) integral would be unavoidable in a computational application. The singularity in a PV integral could be removed by Cauchy's residue theorem. The shallow water Green's function of uniform flow was modified by Sahin and Hyman [3] and was used in the flow simulation of the uniform motion of a submerged body presented by Sahin et al. [4]. The source in parallel planes and rectangular channels was developed by the image method, a restricted domain Green's function can be obtained by distribution of sources along the length of a normal line to the planes and by formal summation of the Green's functions in the computational domain. Infinite series arising from the application of image methods are slowly convergent [2,4,5]. Different remedies have been introduced to change these series of images into rapidly convergent formulations. The Green's function of a channel water-wave with infinite depth was obtained by Kashiwagi [6] in which slowly convergent series were transformed by a double integral over a semi-infinite domain. The 3D acoustic Green's function in a rectangular channel was given by Newman [7] in which sources in two transverse directions were distributed, and Fourier techniques were applied to transform an infinite series of images into an applied Green's function. Oscillating source problems in channels with infinite and finite depth were solved by Linton [5]. For infinite and finite depth, the slowly convergent series were rewritten into a rapidly convergent series by Eigen function expansion. For finite depth channels, orthonormal sets of functions are also adopted. A suitable Green's function is proposed by Xia [8] for 3D wave-body interaction problems in the channels. This formulation is based on the open-sea Green's function. The infinite series of images are evaluated through the asymptotic analysis. Solutions of a 3D acoustic source in parallel planes and an infinite open rectangular prism were expressed as a series of images by Ismail and Elbenhady [9]. They used the Eigen function expansions to transform slowly convergent series into an integral representation, which is rapidly convergent and stable.

Numerical tanks have been developed since the past two decades to compute flow field around objects in presence of the free surface. Potential numerical tank has been based on boundary integral equation and MEL (Mixed Eulerian-Lagrangian) method. Free surface is included in boundary integral explicitly, and its mutations have been obtained through transforming free surface boundary condition from Eulerian form into Lagrangian form. A 2D wave-current interaction was investigated by Ryu et al. [10], and 3D wave-current interaction modeling was carried out by Zhen and Bin [11]. In these numerical tanks, 2D and 3D acoustic Green's function are distributed over the free surface and inflow and outflow boundaries to satisfy the radiation condition in the integral equation. So, computations are time-consuming with numerical errors. Also, the description of the free surface fluctuation is complicated.

Dawson method has been applied in direct and indirect BIE (Boundary Integral Equation) to study the effect of free surface on fluid flow around moving, floating and submerged bodies. The performance of moving 3D hydrofoil was examined by Xie and Vassalas [12]. Applying free surface boundary condition to BIE is a little tricky and too sensitive to the size and shape of the free surface grids. Therefore, this scheme is not reliable for practical approaches.

An efficient and accurate technique was proposed by Scullen and Tuck [13] to compute a 3D fundamental solution of uniformly and non-uniformly distribution of moving pressure patches for far field and near field domain. The multiple expansions were applied to the 3D free surface Green's function of oscillation source by Borgarino et al. [14]. It is pointed out that the recently mentioned Green's functions have been practiced in open-sea condition. Hence, the achievement of a practical 3D free surface Green's function of restricted condition for an NTT could be useful.

In the present work, Green's function of a source with constant strength in a uniform flow is evaluated for a rectangular tank with arbitrary dimensions. The boundary conditions contain linearized free-surface conditions, impermeable boundary conditions on the bottom and side walls, and the radiation condition. Open-sea finite-depth Green's function will be adopted in the evaluation procedure. The proposed Green's function includes the mentioned boundary conditions, except the side walls boundary condition. Numerical towing tank Green's function would be approximated by distribution of images of the source on the length of normal direction of the wall and formal summation of the Green's functions on the computational domain. The Green's function of a practical numerical towing tank is aimed in this study. For this purpose, this infinite series will be discrete in three parts. The first part includes the slowly convergent series of the $1/r$ term. In the second and third parts, the integrals of infinite series are approximated. The rapidly convergent form of the first part can be obtained

based on Eigen function expansions. Cauchy's integral theorem and Poisson's summation formula combined with a convergent geometric series are employed to compute the principle value integrals in the series of the second part. In the same manner, the definite integral in the series of the third term is evaluated. The dependency of the flow properties to width and depth of the tank are shown and verified by the modified open-sea free-surface Green's function. Modeling of a uniform motion of a submerged sphere and ellipsoid in a numerical towing tank are developed on the basis of the constant panel method. Simulation of fluid flow around a sphere is compared with analytical solutions and other numerical results. Center plane wave profiles of a sphere and an ellipsoid are obtained to study the effects of tank width on the solution for various tank dimensions and different flow regimes.

2. Background

The Cartesian coordinates system is chosen with the (x, y) plane on the undisturbed free surface, and z is measured vertically upwards. The width of the tank is W and its depth is h as shown in Figure 1. Fluid is assumed to be inviscid and incompressible, and the flow is irrotational. Therefore, the Laplace equation is the governing equation in the computational domain (Ω).

Fluid flow around a body that moves uniformly in the towing tank in $+x$ direction could be computed by potential theory. Hence, velocity potential (Φ) is composed of the uniform flow velocity potential in $-x$ direction, and perturbation velocity potential induced by the existence of the body.

$$\Phi(x, y, z) = \underbrace{-U.x}_{\text{Uniform flow potential}} + \underbrace{\phi(x, y, z)}_{\text{Perturbation potential}}. \quad (1)$$

To compute the perturbation potential, the panel method based on Green's second identity is applied. The direct boundary integral equation for perturbation potential can be written as:

$$\iint_S \left[\phi \frac{\partial G}{\partial n_s} - G \frac{\partial \phi}{\partial n_s}\right] dS = \varepsilon(P)\phi(P), \quad (2)$$

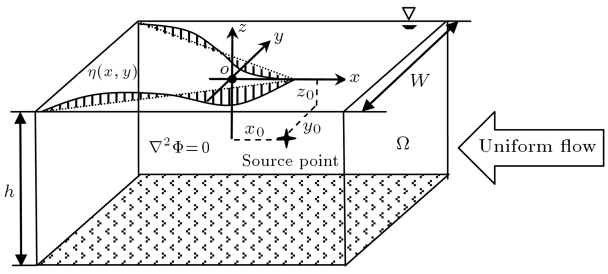

Figure 1. Cartesian system and tank geometry.

where P is a field point positioned on the body surface, walls, bottom or in the fluid domain; S is the control surface of a numerical towing tank, and $\vec{n}$ is the normal vector on a control surface directed into the fluid. The value of ε depends on the location of the field point. Green's function (G) is the solution of Eq. (3) that must satisfy the boundary conditions.

$$\nabla^2 G = \delta(x - x_0)\delta(y - y_0)\delta(z - z_0) \quad \text{in} \quad \Omega, \quad (3)$$

where δ is the Dirac delta function. Indeed, a constant strength source in uniform flow at (x_0, y_0, z_0) disturbs the whole fluid flow domain (x, y, z). Green's function represents the source disturbance affected by a set of boundary conditions. NTT boundary conditions contain the following.

Free surface boundary condition: Free surface elevation $\eta(x, y)$ is measured from the calm water level. This boundary condition is made of a combination of dynamic and kinematics boundary conditions.

$$\frac{\partial^2 G}{\partial x^2} + K_0 \frac{\partial G}{\partial z} = 0, \qquad \text{on} \quad z = 0, \quad (4)$$

where $K_0 = g/U^2$.

Bottom condition: The tank bottom is impermeable and its slope is zero; therefore, the normal derivative of the Green's function must be considered as to be zero:

$$\frac{\partial G}{\partial z} = 0 \quad \text{on} \quad z = -h. \quad (5)$$

Radiation condition: To ensure that the disturbance wave would shrink upstream and to obtain a unique solution for the boundary value problem, the radiation condition is applied:

$$\lim_{r^2 \to \infty} G = O(1), \qquad \text{for} \quad x < 0,$$

$$\lim_{r^2 \to \infty} G = 0, \qquad \text{for} \quad x > 0, \quad (6)$$

where:

$$r = \sqrt{(x - x_0)^2 + (y - y_0)^2 + (z - z_0)^2}.$$

Tank's wall condition: The normal derivative of the fundamental solution must be zero, owing to the impermeable walls of the tank:

$$\frac{\partial G}{\partial y} = 0 \quad \text{on} \quad y = \pm \frac{W}{2}. \quad (7)$$

If the solution of Eq. (3) satisfies the NTT boundary conditions, the control surface in Eq. (2) is limited to the body surface.

3. Formulation of Green's function

The open-sea Green's function in the finite depth for a constant strength source located at $(0, 0, z_0)$ given by Wehausen and Laitone [1] can be rewritten as:

$$G_o = -I_1 + \frac{4}{\pi} I_2 + 4I_3. \tag{8}$$

The term I_1 represents the source and its image with respect to the bottom. The term I_2 indicates the free surface disturbance due to the presence of the source, and its image and the term I_3 exists to satisfy the radiation condition [15].

For $K_0 h > 1$,

$$I_1 = \frac{1}{r_1} + \frac{1}{r_2}, \tag{9}$$

where:

$$r_1^2 = x^2 + y^2 + (z - z_0)^2,$$

$$r_2^2 = x^2 + y^2 + (z + (2h + z_0))^2,$$

and:

$$I_2 = PV \int_0^{\infty} \int_0^{\pi/2} F(\theta, k, z) \cos(kx \cos\theta) \times \cos(ky \sin\theta) d\theta dk, \tag{10}$$

where:

$$F(\theta, k, z) = \frac{e^{-kh} \cosh[k(h + z_0)](k + K_0 \sec^2\theta)}{\cosh(kh)(k - K_0 \sec^2\theta \tanh(kh))} \times \cosh(k(h + z)),$$

and:

$$I_3 = \int_0^{\pi/2} H(\theta, K, z) \sin(Kx \cos\theta) \cos(Ky \sin\theta) d\theta, \tag{11}$$

where:

$$H(\theta, K, z) = \frac{e^{-Kh} \cosh[K(h + z_0)](K + K_0 \sec^2\theta)}{\cosh(Kh)(1 - K_0 \sec^2\theta \sec h^2(Kh))} \times \cosh(K(z + h)).$$

In function F, k is integration variable and in function H, K is the wave number which can be determined by Eq. (12):

$$K - K_0 \sec^2\theta \tanh(Kh) = 0. \tag{12}$$

3.1. Image method

To use the image method, the walls of the tank are removed, and the control volume becomes unbounded in the transverse direction. Instead, an infinite series of the images of the source are distributed over the normal axis to the walls of the tank, as shown in Figure 2. According to Figure 2, the position of the images in the y direction in an unbounded domain can be written as:

$$y_0' = y_0 + 2nW, \qquad n = -\infty \cdots \infty,$$

$$y_0'' = -y_0 + (2n + 1)W, \qquad n = -\infty \cdots \infty. \tag{13}$$

Green's function for the image of each source can be approximated by substituting its position in Eq. (8). Then, the Green's function of the tank can be expressed by formal summation of these infinite Green's functions as:

$$G = -\underbrace{\sum_{n=-\infty}^{\infty} (I_1' + I_1'')}_{J_1} + \frac{4}{\pi} \underbrace{\sum_{n=-\infty}^{\infty} (I_2' + I_2'')}_{J_2} + 4 \underbrace{\sum_{n=-\infty}^{\infty} (I_3' + I_3'')}_{J_3}, \tag{14}$$

where J_1 represents source and its images with respect to the walls of the tank and the bottom of the tank.

$$J_1 = \sum_{n=-\infty}^{\infty} \left[\frac{1}{r_1'} + \frac{1}{r_1''} + \frac{1}{r_2'} + \frac{1}{r_2''} \right], \tag{15}$$

in which:

$$r_1'^2 = (x - x_0)^2 + (y - y_0')^2 + (z - z_0)^2,$$

$$r_1''^2 = (x - x_0)^2 + (y - y_0'')^2 + (z - z_0)^2,$$

$$r_2'^2 = (x - x_0)^2 + (y - y_0')^2 + (z + (2h + z_0))^2,$$

$$r_2''^2 = (x - x_0)^2 + (y - y_0'')^2 + (z + (2h + z_0))^2.$$

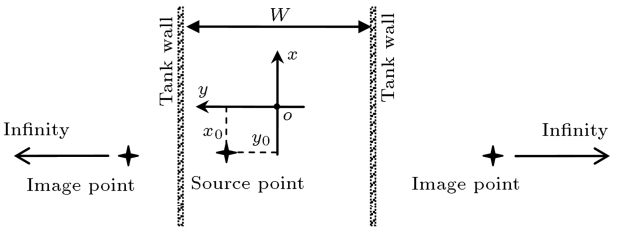

Figure 2. Image method scheme with respect to the tank walls.

The second and third term (J_2, J_3) could be re-written in complex space as follows:

$$J_2 = \mathrm{Re}\Bigg\{ \sum_{n=-\infty}^{\infty} PV \int_0^{\infty} dk \int_0^{\pi/2} F(\theta,k,z)\cos[k(x-x_0)\cos\theta] \times \Big[e^{ik(y-y_0+2nW)\sin\theta} + e^{ik(y+y_0+W+2nW)\sin\theta}\Big]\, d\theta \Bigg\}$$

$$= \mathrm{Re}\Bigg\{ PV \int_0^{\infty} dk \sum_{n=-\infty}^{\infty} \int_0^{\pi/2} [F_1(\theta,k,x,y,z) + F_2(\theta,k,x,y,z)] \times e^{ik2nW\sin\theta} d\theta \Bigg\}, \quad (16)$$

in which:

$$F_1(\theta,k,x,y,z) = F(\theta,k,z)\cos[k(x-x_0)\cos\theta] e^{ik[y-y_0]\sin\theta},$$

$$F_2(\theta,k,x,y,z) = F(\theta,k,z)\cos[k(x-x_0)\cos\theta] e^{ik[y+y_0+W]\sin\theta},$$

and:

$$J_3 = \mathrm{Re}\Bigg\{ \sum_{n=-\infty}^{\infty} \int_0^{\pi/2} G(\theta,K,z)\sin[K(x-x_0)\cos\theta] \times \Big[e^{iK(y-y_0+2nW)\sin\theta} + e^{iK(y+y_0+W+2nW)\sin\theta}\Big] d\theta \Bigg\}$$

$$= \mathrm{Re}\Bigg\{ \sum_{n=-\infty}^{\infty} \int_0^{\pi/2} [G_1(\theta,K,x,y,z) + G_2(\theta,K,x,y,z)] \times e^{iK2nW\sin\theta} d\theta \Bigg\}, \quad (17)$$

where:

$$G_1(\theta,K,x,y,z) = G(\theta,K,z)\sin[K(x-x_0)\cos\theta] e^{iK[y-y_0]\sin\theta},$$

$$G_2(\theta,K,x,y,z) = G(\theta,K,z)\sin[K(x-x_0)\cos\theta] e^{iK[y+y_0+W]\sin\theta}.$$

3.2. Asymptotic analysis for J_1

Slow convergence of the series in Eq. (15) causes difficulties in numerical applications [2,16]. The Eigen function expansions and their deriving approaches given by Ismail and Elbenhady [9] are adopted to obtain an applicable form of J_1. For a singularity $1/r$ in the middle of parallel planes, the Green's function ($\bar{G}$) is written as [16]:

$$\bar{G}(\rho,y;\sigma) = (\rho^2+y^2)^{-1/2} + \sum_{\substack{m=-\infty \\ m\neq 0}}^{\infty} \Big\{ \big[\rho^2 + (y-m\sigma)^2\big]^{-1/2} - |m\sigma|^{-1} \Big\}, \quad (18)$$

where σ is the width of parallel planes, and $\rho = \sqrt{x^2+z^2}$. In the infinite series in Eq. (18), $|m\sigma|^{-1}$parameter, as a constant, is subtracted from each term of fundamental solution to reach to the convergent series. Using the Eigen function expansions can make the Green's function be more rapidly convergent. An alternative form of Eq. (18) is given as [16]:

$$\bar{G}(\rho,y) = -2\left(C + \ln\frac{\rho}{2}\right) + 4\sum_{m=1}^{\infty} k_0(2\pi m\rho)\cos(2\pi m y), \quad (19)$$

where $C = 0.577215665$ is the Euler's constant given by Gradshteyn and Ryzhik [15], and k_0 is the modified Bessel function of the second kind of order zero. In Eq. (15), the four slow convergent infinite series of singularities can be written for $\sigma \equiv 2W$.

$$S_1 = \big((x-x_0)^2 + (y-y_0)^2 + (z-z_0)^2\big)^{-1/2} + \sum_{\substack{n=-\infty \\ n\neq 0}}^{+\infty} \Big\{ \big[(x-x_0)^2 + (z-z_0)^2 + (y-y_0-2nW)^2\big]^{-1/2} - |2nW|^{-1} \Big\}, \quad (20)$$

$$S_2 = \big((x-x_0)^2 + (y-y_0-W)^2 + (z-z_0)^2\big)^{-1/2} + \sum_{\substack{n=-\infty \\ n\neq 0}}^{+\infty} \Big\{ \big[(x-x_0)^2 + (z-z_0)^2 + (y+y_0-W-2nW)^2\big]^{-1/2} - |2nW|^{-1} \Big\}, \quad (21)$$

$$S_3 = \big((x-x_0)^2 + (y-y_0)^2 + (z+(2h+z_0))^2\big)^{-1/2} + \sum_{\substack{n=-\infty \\ n\neq 0}}^{+\infty} \Big\{ \big[(x-x_0)^2 + (z+(2h+z_0))^2 + (y-y_0-2nW)^2\big]^{-1/2} - |2nW|^{-1} \Big\}, \quad (22)$$

$$S_4 = \left((x-x_0)^2+(y+y_0-W)^2+(z+(2h+z_0))^2\right)^{-1/2} + \sum_{\substack{n=-\infty \\ n\neq 0}}^{+\infty} \Big\{ \left[(x-x_0)^2+(z+(2h+z_0))^2 + (y+y_0-W-2nW)^2\right]^{-1/2} - |2nW|^{-1} \Big\}. \quad (23)$$

By substituting Eqs. (20)-(23) into Eq. (19), four rapidly convergent series are obtained. For example, S_1 series can be written in the following form:

$$S_1 = -2\left(C+\ln\frac{\sqrt{(x-x_0)^2+(z-z_0)^2}}{2}\right) + 4\sum_{m=1}^{\infty} B_0\left(2\pi m\sqrt{(x-x_0)^2+(z-z_0)^2}\right) \cos\left[2\pi m(y-y_0)\right]. \quad (24)$$

Other series can be transformed in the same manner. Formal summation of convergent series S_1, S_2, S_3, S_4 makes a unique series for application in numerical computation.

3.3. Modifying analysis for J_2 and J_3

Simplification of J_2 and J_3 from the integral series to a simpler form can be carried out by the Poisson summation formula described in general form as:

$$S_N = \sum_{n=-\infty}^{\infty}\int_a^b E(\theta)e^{\inf(\theta)}d\theta = \int_a^b E(\theta)\sum_{n=-\infty}^{\infty} e^{\in f(\theta)}d\theta, \quad (25)$$

where $E(\theta)$ is an arbitrary function. Using a convergent geometric series given by Gradshteyn and Ryzhik [15], we have:

$$\sum_{n=-N}^{N-1} e^n = \frac{e^N-e^{-N}}{e-1}, \quad (26)$$

and substituting Eq. (26) into Eq. (25), we have:

$$S_N = \int_a^b F(\theta)\frac{\left[e^{iNf(\theta)}-e^{-iNf(\theta)}\right]}{e^{if(\theta)}-1}d\theta, \quad \text{when} \quad N\to\infty, \quad (27)$$

where $F(\theta)$ is an arbitrary function and the integrand has poles on $\theta_m = \pm 2m\pi$. Taylor expansion of f function for $\theta = \theta_m + p$ can be written as:

$$f(\theta) = f(\theta_m)+pf'(\theta_m)+p^2/2f''(\theta_m)+\cdots \approx 2m\pi + pf'(\theta_m). \quad (28)$$

Thus:

$$e^{if(\theta)}-1 = e^{ipf'(\theta_m)} \approx ipf'(\theta_m), \qquad \text{as} \quad p\to 0. \quad (29)$$

There might be a number of such poles at $[a,b]$ in Eq. (27) when $N\to\infty$. If each pole has the vicinity $(-\varepsilon,\varepsilon)$, then Eq. (27) can be obtained as:

$$S_N = \sum_m \int_{-\varepsilon}^{\varepsilon} F(\theta_m)\frac{\left[e^{iNpf'(\theta_m)}-e^{-iNpf'(\theta_m)}\right]}{ipf'(\theta_m)}dp. \quad (30)$$

By substituting:

$$u = Npf'(\theta_m),$$

$$du = Nf'(\theta_m)dp,$$

$$R = N\varepsilon f'(\theta_m).$$

Eq. (31) can be achieved.

$$S_N = {\sum_m}' \pm\frac{F(\theta_m)}{if'(\theta_m)}\int_{-R}^{R}\frac{[e^{iu}-e^{-iu}]}{u}du \quad \begin{bmatrix} + & f'(\theta_m)>0 \\ - & f'(\theta_m)<0 \end{bmatrix} = {\sum_m}'\frac{2\pi F(\theta_m)}{|f'(\theta_m)|}, \quad (31)$$

where $\sum'$ denotes that if $\theta = a$ or $\theta = b$, the term $m = 0$ must be halved. In the same manner, Eqs. (16) and (17) can be modified for $(0 \le \theta \le \pi/2)$, and the modified form of the equations can be written as:

$$J_2 = \mathrm{Re}\Big\{ PV\int_0^{\infty} dk\frac{\pi}{W}{\sum_{m=0}^{\infty}}'\frac{F(\theta_m,k,z)}{k\cos\theta_m} \times \cos(kx\cos\theta_m)e^{iky\sin\theta_m} \left[e^{-iky_0\sin\theta_m}+(-1)^m e^{iky_0\sin\theta_m}\right]\Big\}$$

$$= \frac{2\pi}{W}PV\int_0^{\infty} dk\frac{\pi}{W}{\sum_{m=0}^{\infty}}'\frac{F(\theta_m,k,z)}{k\cos\theta_m} \times \cos(kx\cos\theta_m) \times \begin{cases}\cos(ky\sin\theta_m)\cos(ky_0\sin\theta_m)\\ \sin(ky\sin\theta_m)\sin(ky_0\sin\theta_m)\end{cases} \quad (32)$$

in which cos and sin depend on the odd and even value of m, respectively, and $k\sin\theta_m = m\pi/W$.

$$J_3 = \frac{2\pi}{W}\sum_{m=0}^{\infty}{}' \frac{e^{-K_m h}(K_0 + K_m\cos^2\theta_m)}{(1 - K_0 h\sec h^2(K_m h) + \sin^2\theta_m)} \times \frac{\cosh(K_m(z+h))}{\cosh(K_m h)}\cosh(K_m(z_0+h)) \times \frac{\sin(K_m(x-x_0)\cos\theta_m)}{K_m\cos\theta_m} \times \begin{cases}\cos(K_m y\sin\theta_m)\cos(K_m y_0\sin\theta_m)\\ \sin(K_m y\sin\theta_m)\sin(K_m y_0\sin\theta_m)\end{cases} \quad (33)$$

Also, cos and sin depend on the odd and even value of m, respectively, and $K_m\sin\theta_m = m\pi/W$.

3.4. Evaluation of the principal value integral in J_2

In general, Cauchy principal value integral could be introduced for the first order pole as follows:

$$I = \lim_{|x|\to\infty}\int_a^b \frac{D(k)}{k-K}e^{id(k)x}dk = \pm\pi i D(K)e^{id(K)x}, \quad (34)$$

in which the $-$ sign is for $x < 0$ and the $+$ sign is for $x > 0$. Function g is defined as follows:

$$g(k) = k - K_0\sec^2\theta_m\tanh(kh) = 0. \quad (35)$$

Using a derivative of function g with respect to k and $k\sin\theta_m = m\pi/W$, the Taylor expansion of this function can be written as:

$$g(k) = g'(K)(k-K) = (1 - K_0 h\sec^2\theta_m\sec h^2(Kh) + 2K_0\tan^2\theta_m\sec^2\theta_m\tanh(Kh)/K)(k-K) = \sec^2\theta_m(1 - K_0 h\sec h^2(Kh) + \sin^2\theta_m)(k-K). \quad (36)$$

It can be shown that $K = K_m$ for $K_m\sin\theta_m = m\pi/W$. If function D and function d are defined as:

$$D(K_m) = \frac{e^{-K_m h}\cosh[K_m(h+z_0)]}{(1 - K_0 h\sec h^2(K_m h) + \sin^2\theta_m)} \times (K_0 + K_m\cos^2\theta)\frac{\cos[K_m(z+h)]}{\cosh(K_m H)} \times \frac{1}{K_m\cos\theta_m} \times \begin{cases}\cos(ky\sin\theta_m)\cos(ky_0\sin\theta_m)\\ \sin(ky\sin\theta_m)\sin(ky_0\sin\theta_m)\end{cases} \quad (37)$$

$$d(K_m) = K_m\cos\theta_m, \quad (38)$$

then the principal value integral, J_2, can be calculated as:

$$J_2 = \frac{2\pi}{W}\sum_{m=0}^{\infty}{}'\{\text{Real}(I)\} = \frac{2\pi}{W}\sum_{m=0}^{\infty}{}'\{\pm\pi D(K_m)\sin(K_m(x-x_0)\cos\theta_m)\} = \pm\frac{2\pi^2}{W}\sum_{m=0}^{\infty}{}'\frac{e^{-K_m h}(K_0 + K_m\cos^2\theta_m)}{(1 - K_0 h\sec h^2(K_m h) + \sin^2\theta_m)} \times \frac{\cosh(K_m(z_0+h))}{\cosh(K_m h)}\cosh(K_m(z+h)) \times \frac{\sin(K_m(x-x_0)\cos\theta_m)}{K_m\cos\theta_m} \times \begin{cases}\cos(K_m y\sin\theta_m)\cos(K_m y_0\sin\theta_m)\\ \sin(K_m y\sin\theta_m)\sin(K_m y_0\sin\theta_m)\end{cases} \quad (39)$$

4. Analysis of results

The efficient free-surface Green's function in a numerical towing tank is developed in this paper. The open-sea Green's function and image method are employed to obtain an appropriate NTT Green's function. Asymptotic analysis based on Eigen function expansions and the Cauchy principal value integral associated with the Poisson summation formula are applied to remove computational singularities (i.e. slow convergent infinite series in the principal value integral).

Usually, the physical towing tank is used to test models in open-sea and restricted water conditions. Therefore, the NTT Green's function must be tested and be able to model the open-sea and restricted water conditions. In the following, numerical computation of NTT Green's function is carried out for two case studies, i.e. uniform motion of a submerged sphere and an ellipsoid. Added mass and the distribution of potential over the body sphere in open-sea conditions are calculated and compared with the analytic and numerical solutions. The effect of the wall of the tank on the free-surface disturbance induced by a sphere and an ellipsoid motion in the tank is also investigated.

4.1. Towing tank Green's function verification

The towing tanks have been widely used to determine fluid flow and hydrodynamic resistance for the bodies moving in the open-sea and restricted water conditions. Figure 3 shows the results of the proposed towing tank Green's function and the open-sea Green's function of a singularity located at $(0, 0, -f)$ in the uniform flow proposed by Sahin and Hyman [3]. The submergence depth parameter of a source point is defined by $\alpha =$

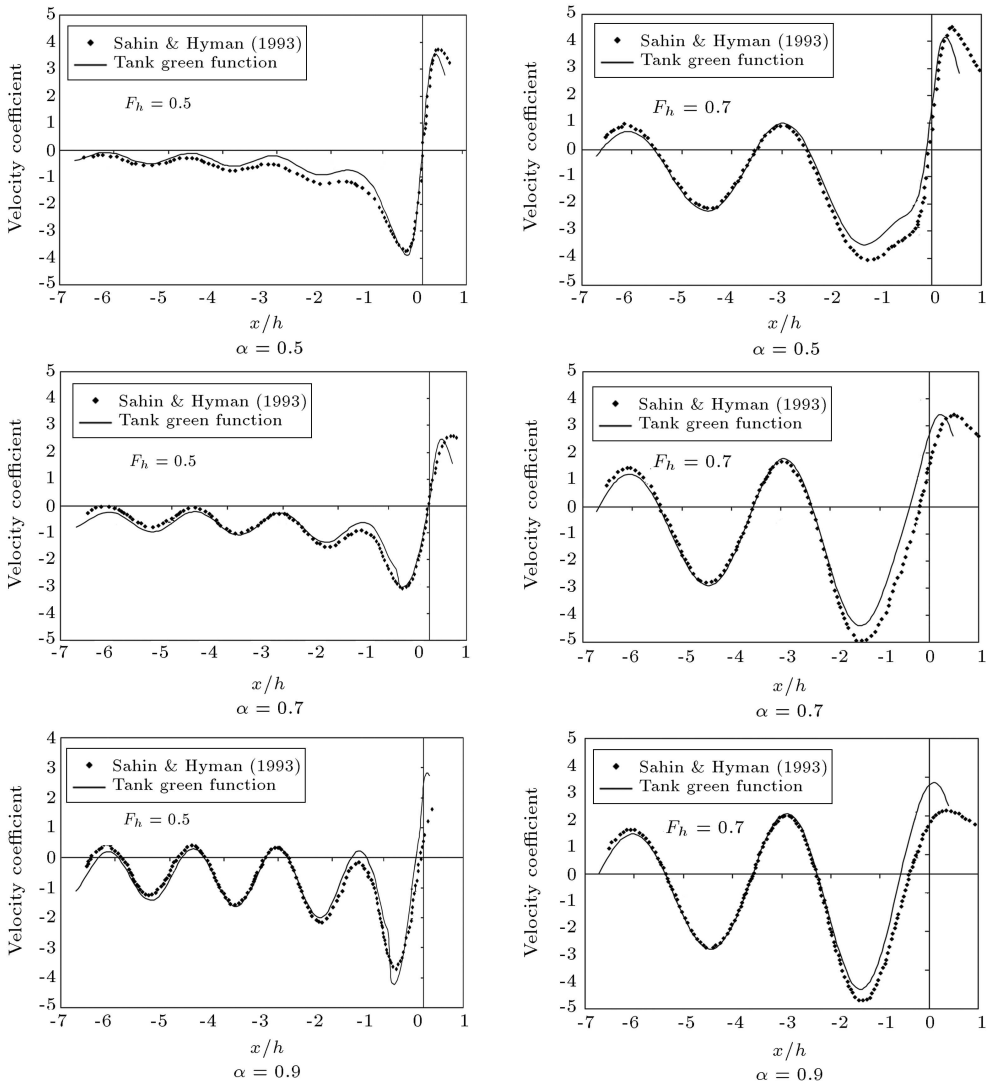

Figure 3. Comparison of velocity coefficient of a source in the open-sea condition.

$(h - f)/h$, and the depth Froude number is defined as $F_h = U/\sqrt{gh}$. Velocity coefficient is $\chi = (\partial G/\partial x)h^2/m$ in which m is the source strength computed at $(y = 0, z = -h)$. Velocity coefficient is calculated in two flow regimes ($F_h = 0.5, 0.7$) and different submergence depth parameters of the sources. It is worth mentioning that the width of the towing tank is taken very large ($1000h$) for the comparison of the results obtained by the modified Green's function and the results reported by Sahin and Hyman [3].

The disturbance wave pattern can be approximated through the linearized dynamic free-surface boundary condition as below:

$$\eta = U\frac{\partial G}{\partial x}. \tag{40}$$

Wave propagation in open-sea state induced by the existence of a source point in uniform flow is illustrated over half of the domain in Figure 4 for two different flow regimes (different depth Froude number) and a constant submergence depth parameter. It is shown that a wave pattern for a constant submergence depth parameter is severely affected by flow regimes. The amplitude of wave is increased, and waves are propagating divergently as the uniform flow velocity is increased. The wave pattern for a source point with a constant depth Froude number (F_h) and different depth parameter (α) is illustrated in Figure 5. It shows that when submergence depth parameter is increased, the disturbance wave amplitude enlarges and wave pattern diverges.

Reflected waves from the walls of the tank are essential for the investigation of the effect of walls on the free-surface disturbance and capability of the image method to model the tank walls boundary condition. Figure 6 shows the wave pattern of a source point located at a constant depth parameter under the different flow regimes in a towing tank. Meanwhile,

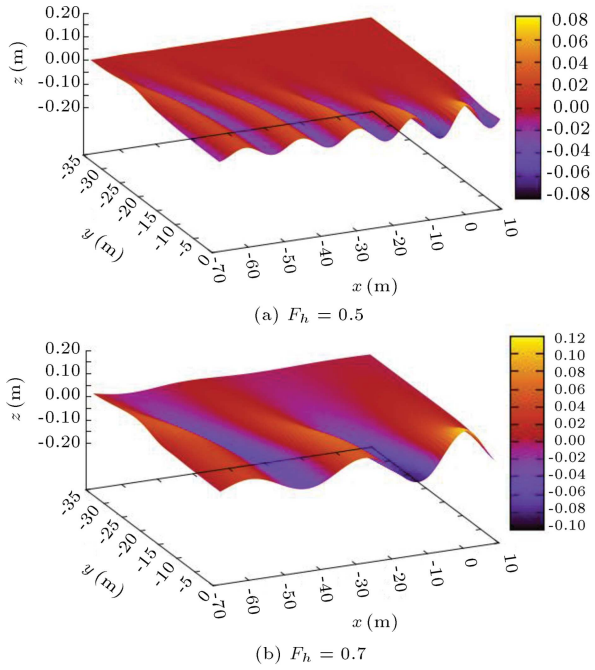

Figure 4. Disturbance wave pattern of a source in the different flow regimes (depth Froude number) at $\alpha = 0.5$.

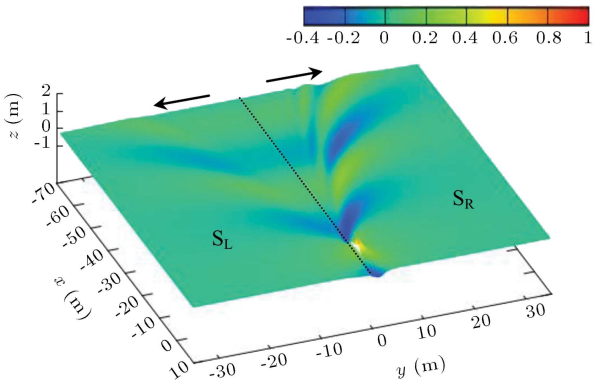

Figure 5. Wave pattern comparison of a source in a constant flow regime ($F_h = 0.7$) and various α; SL ($\alpha = 0.7$), SR ($\alpha = 0.9$).

when the wave pattern is more divergent, the fully developed reflected wave field is beginning farther than the source point.

4.2. Numerical examples

The modified towing tank Green's function is applied in a numerical computation of the motion of a sphere and an ellipsoid in NTT. The distribution of the velocity potential over a sphere and the surge added mass (m_{11}) are computed and compared with the analytical solutions and the existing numerical results. In this study, the direct boundary integral method is used to compute potential fluid flow. The body surface is described by triangle panels as shown in Figure 7.

The towing tank Green's function is substituted in

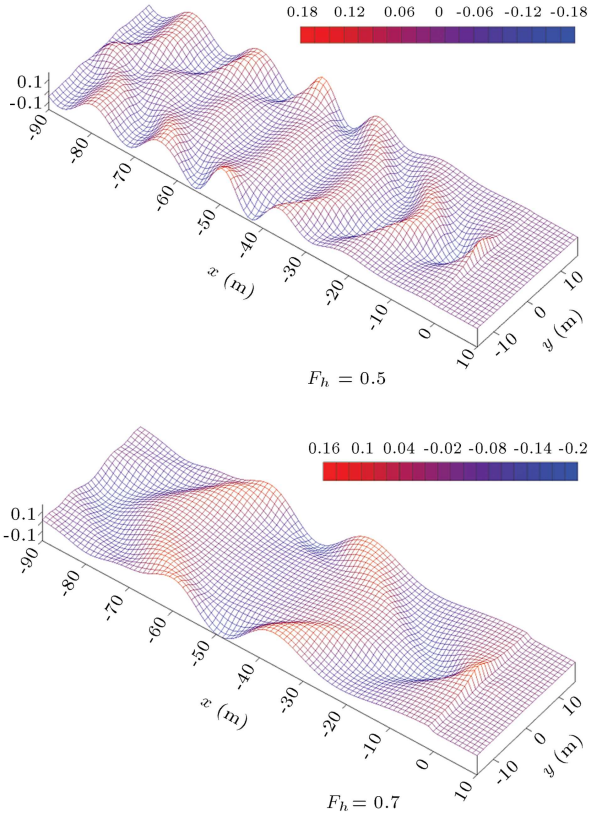

Figure 6. Wave pattern of a source in the NTT with a constant submergence depth parameter ($\alpha = 0.7$) and the tank's width 30 (m) at various flow regimes.

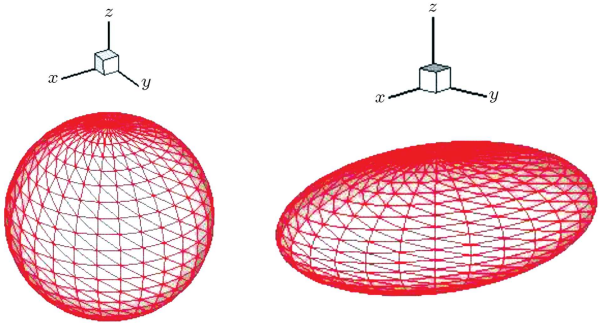

Figure 7. Triangle meshes over the body surface.

the Green's formula for modeling the uniform motion of a floating or submerged body in the numerical towing tank. The second Green's identity is written as:

$$\iint_{S_q} \left[\phi_q \frac{\partial G_{P_q}}{\partial n_q} - G_{P_q} \frac{\partial \phi}{\partial n_q}\right] dS_q = \varepsilon(P)\phi(P), \qquad (41)$$

where P is a field point, q is a source point, and S_q indicates body surface. $\varepsilon(P)$ depends on the position of the field point, which can be located on the body surface ($\varepsilon(P) = 2\pi$) or in the control volume ($\varepsilon(P) = 4\pi$) or out of the domain ($\varepsilon(P) = 0$). The constant

panel method is used in the numerical computation. The distribution of velocity potential over the panels is assumed to be constant, and the source point is located at the center of each panel. On each panel, the normal flux of potential (body boundary condition) is the known value, and the potential is the unknown value that must be calculated. Impermeable body condition is expressed as:

$$\frac{\partial \Phi}{\partial n}\Big)_{S_q} = 0 \rightarrow \frac{\partial \phi}{\partial n}\Big)_{S_q} = Un_x, \tag{42}$$

in which n_x is x coordinate of body unit normal vector directed into the fluid. The descritized form of Eq. (41) can be written as:

$$\sum_{j=1}^{N}\left[\phi_j \iint_{S_j} \frac{\partial G_{ij}}{\partial n_j} dS_j + 2\pi\phi_j\delta_{ij}\right] = \sum_{j=1}^{N}\iint_{S_j} G_{ij} U\vec{i}.\vec{n}_j dS_j, \tag{43}$$

where δ is Kronecker delta function, and j indicates the number of panels and i shows the field point. Eq. (43) is an algebraic system of equations with unknown values on the left hand side and the vector of known values on the right side of equation.

The uniform motion of a sphere with radius r and $U = 1m/s$ in an unbounded fluid is simulated. Determination of perturbation potential on the sphere body is verified by computation of the surge added mass (m_{11}) and distribution potential over the body surface. The added masses are defined as:

$$m_{ij} = \rho, \iint_{S_q} \phi_j \frac{\partial \phi_j}{\partial n} dS, \qquad i, j = 1, 2, \cdots 6. \tag{44}$$

Table 1 shows the result of computation of the surge added mass, using the proposed Green's function and the exact solution. It is shown that accurate results can be obtained by present Green's function. However, increase in the number of panels results in decrease in the error of computation.

The distribution of velocity potential over the sphere is calculated in unrestricted water to prove the simulation in this numerical towing tank. The radius of the sphere is taken to be 1 and the unbounded uniform flow is from $-x$ direction with its speed $U = 1m/s$. The perturbation potential along the polar angle, $\theta = 0$ deg. to $\theta = 90$ deg., at the y plane on sphere surface are computed and compared with the exact solution and Kim and Shin calculations [17] in Figure 8. To compare the results with Kim and Shin [17], the computation is conducted for the tank with very large dimensions ($h = 100f$, $W = 1000h$).

Furthermore, the effect of tank width on the surge added mass coefficient ($m_{11}/\pi\rho r^3$) of this unit radius sphere is shown in Figure 9. It was shown that surge added mass was increased severely as tanks width was decreased for a constant depth. The walls of the tank restrict fluid flow around the body and fluid particles are forced to pass the body more quickly by decreasing the tank width.

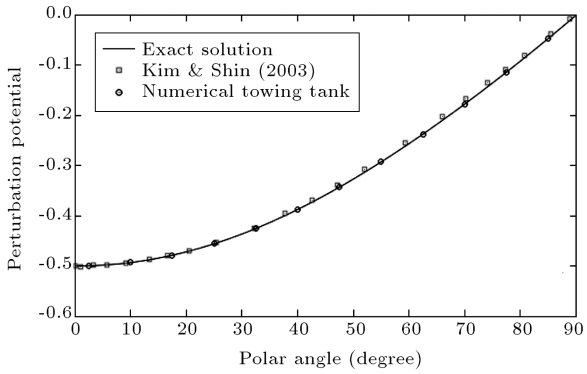

Figure 8. Perturbation potential on the sphere surface.

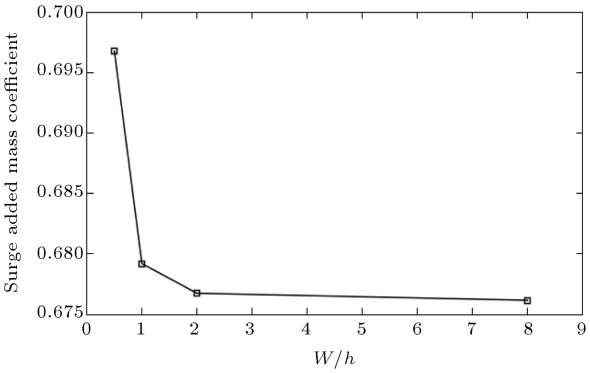

Figure 9. Surge added mass coefficient of the unite radius sphere in the towing tank ($F_h = 0.1$) with various width.

Table 1. The surge added mass of a sphere.

No. of panels	NTT solution of $m_{11}/\pi\rho r^3$	Exact solution of $m_{11}/\pi\rho r^3$	% of error	Abs. error
512	6.7605E-01	6.6667E-01	1.4075E+00	9.3833E-03
768	6.7592E-01	6.6667E-01	1.3880E+00	9.2533E-03
1064	6.6754E-01	6.6667E-01	1.3100E-01	8.7333E-04
1565	6.6700E-01	6.6667E-01	5.0000E-02	3.3333E-04
2048	6.6698E-01	6.6667E-01	4.6499 E-02	3.1000E-04
3072	6.6701E-01	6.6667E-01	5.0999E-02	3.4000E-04

Furthermore, Figure 10 presents a comparison of the dimensionless wave elevation (η/h) of the center plane in an unbounded domain for the various tanks width -to- bodies width W/B in a constant submerged depth parameter and a constant flow regime. Longitudinal length of ellipsoid is $2b$ and transverse length in z direction is $2a$ and in y direction is $2c$.

Contours of wave patterns due to the presence of a sphere and ellipsoid in open-sea conditions with various flow velocities are presented in Figure 11. Submergence depths of bodies are $2(m)$ under the free-surface.

5. Conclusion

The measuring of hydrodynamic characteristics, resistance and analysis of fluid flow for a body mov-

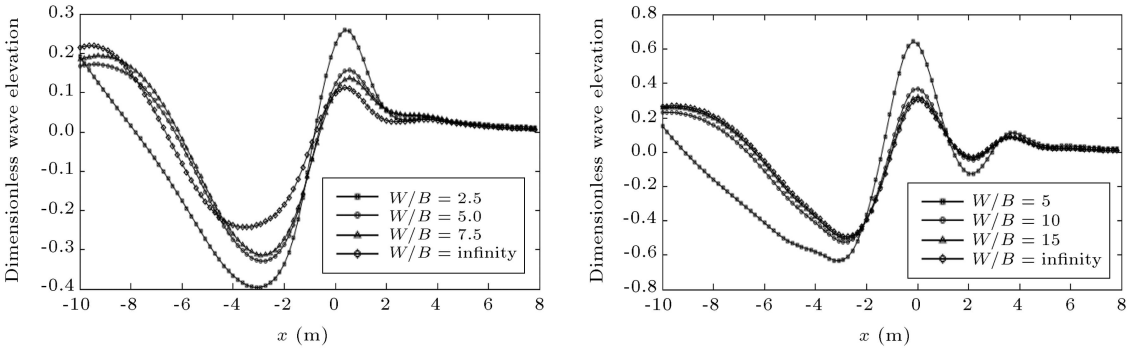

(a) Sphere ($r = 1$) (b) Ellipsoid ($a/b = 0.5$, $c/b = 0.5$)

Figure 10. Comparison of calculated center plane wave profile in unbounded and at various W/B for a sphere and an ellipsoid at $F_h = 0.7$ and $\alpha = 0.5$.

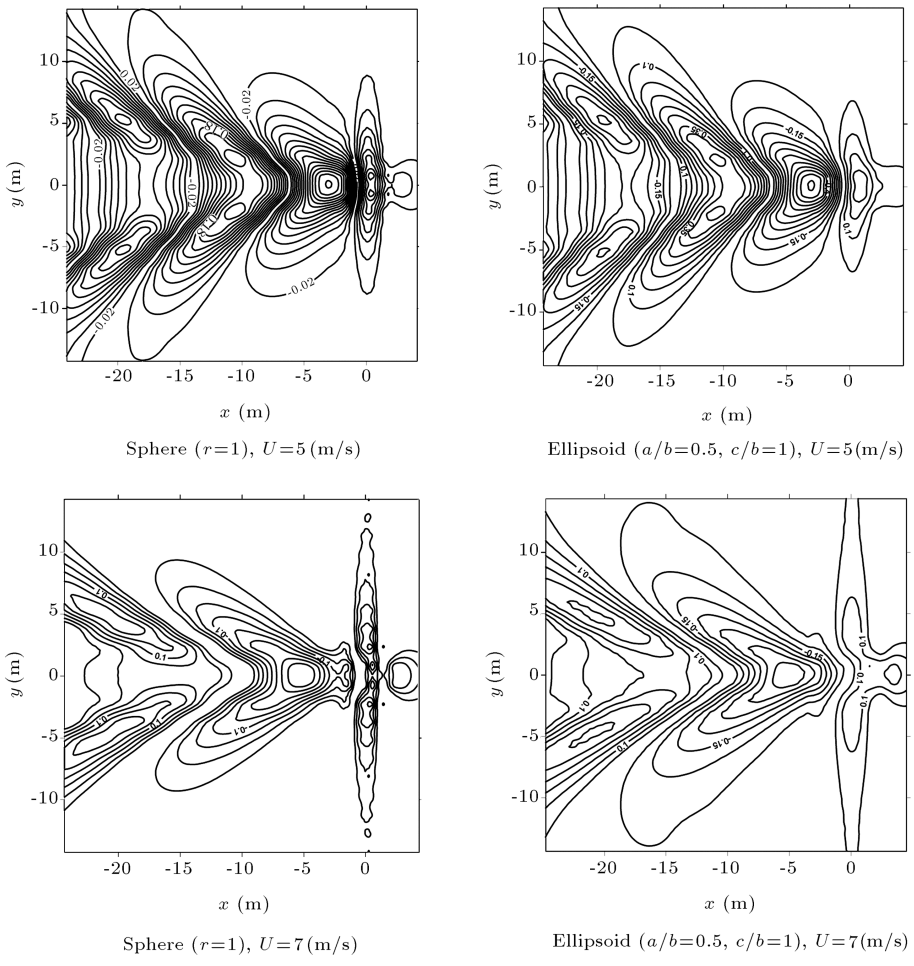

Sphere (r=1), U=5 (m/s) Ellipsoid (a/b=0.5, c/b=1), U=5(m/s)

Sphere (r=1), U=7(m/s) Ellipsoid (a/b=0.5, c/b=1), U=7(m/s)

Figure 11. Wave pattern comparisons due to different flow regimes.

ing uniformly in open-sea conditions or in restricted water conditions are usually carried out by towing tank experiments which could be expensive and time-consuming. Numerical computation is a powerful tool for simulating the motions of a body in NTT. However, accuracy of the results depends on the method and the Green's function used in the computation. Green's function is a fundamental solution of Laplace equation for a constant strength source, which satisfies specific boundary conditions. Free-surface boundary conditions, impermeable bottom and walls of the tank condition, and the radiation condition on upstream of the source are considered in the fundamental solution of towing tank. A modified Green's function for numerical towing tank is developed on the basis of the free surface Green's function for unbounded domain. The NTT Green's function contains infinite slow convergent series and principal value integrals whose numerical application causes difficulties in the solutions. The Eigen function expansions and the Poisson summation formula combined with the Cauchy principal value integral are employed to overcome the difficulties of numerical computation.

Tank walls confine streamline flow around the body, and cause the fluid to travel the body surface more rapidly than in the absence of the tank walls. The flow regime and the width of the tank affect the flow characteristics around the body in the towing tank, and consequently change the free surface disturbance. It could be shown that the wave amplitude was increased when the width of the tank was decreased. Indeed, water accumulation due to the wall and bottom boundary results in the change in the flow streamlines and the increase in water particle velocity and wave making resistance.

References

1. Wehausen, J.V. and Laitone, E.V., *Surface Waves*, Springer-Verlag, New York (1960).
2. Newman, J.N. "Algorithms for the free-surface Green function", *J. Eng. Math.*, **19**, pp. 57-67 (1985).
3. Sahin, I. and Hyman, M. "Numerical calculation for the flow of submerged bodies under a free curface", *Ocean Eng.*, **20**(3), pp. 339-347 (1993).
4. Sahin, I., Hyman, M. and Nguyen, T.C. "Three dimensional flow around a submerged body in finite-depth water", *J. Appl. Math. Model*, **18**, pp. 611-619 (1994).
5. Linton, C.M. "On the free-surface Green's function for channel problems", *Appl. Ocean Res.*, **15**(5), pp. 263-267 (1993).
6. Kashiwagi, M. "Radiation and diffraction forces acting on a three-dimensional body in a narrow tank", *Int. J. Offshore Polar Eng.*, **1**, pp. 101-107 (1991).
7. Newman, J.N. "The Green function for potential flow in rectangular channel", *J. Eng. Math.*, **26**, pp. 377-402 (1992).
8. Xia, J. "Evaluation of the Green function for 3-D wave-body interactions in a channel", *J. Eng. Math.*, **40**, pp. 1-16 (2001).
9. Ismail, I.A. and Elbenhady, E.E. "Green's function for parallel planes and an open rectangular channel-flow", *Math. Comput. Appl.*, **2**(9), pp. 215-224 (2004).
10. Ryu, S., Kim, M.H. and Lynett, P.J. "Fully nonlinear wave-current interactions and kinematics by a BEM-based numerical wave tank", *Comput. Mech.*, **32**, pp. 336-346 (2003).
11. Zhen, L. and Bin, T. "Wave-current interactions with three-dimensional floating bodies", *J. Hydrodynamics*, **22**(2), pp. 229-240 (2010).
12. Xie, N. and Vassalos, D. "Performance analysis of 3D hydrofoil under free surface", *Ocean Eng.*, **34**, pp. 1257-1264 (2007).
13. Scullen, D.C. and Tuck, E.O. "Free-surface elevation due to moving pressure distributions in three dimensions", *J. Eng. Math.*, **70**, pp. 29-42 (2010).
14. Borgarino, M., Babarit, A. and Ferrant, P. "Extension of free-surface Green's function multipole expansion for infinite water depth case", *Int. J. Offshore and Polar Eng.*, **21**(3), pp. 161-168 (2011).
15. Gradshteyn, I.S. and Ryzhik, I.M., *Table of Integrals, Series and Products*, Academic Press, California (2007).
16. Insel, M. and Doctors, L.J. "Wave-pattern prediction of mono hulls and catamarans in a shallow-water canal by linearized theory", In *Proc. 12th Australasian Fluid Mech. Conf.*, New South Wales (1995).
17. Kim, B., and Shin Y.S. "A NURBS panel method for three-dimensional radiation and diffraction problems", *J. Ship Res.*, **47**(2), pp. 177-186 (2003).

Biographies

Arash Abbasnia received his BSc degree in Naval Architecture from Persian Gulf University, Bushehr, and his MSc degree in Offshore Structure from Amirkabir University of Technology, Tehran. He is currently pursuing a PhD degree in Ocean Engineering at Amirkabir University of Technology. His research interests include wave-body interaction, three dimensional numerical wave tank and computational fluid dynamics.

Mahmoud Ghiasi received his BSc degree in Mechanical Engineering from Amirkabir University of Technology, Iran, his MSc degree in Naval Architecture from Technical University of Gdansk, Poland, and his PhD degree from Dalhousie University, Canada. He is currently working as an assistant professor at Amirkabir University of Technology. His research interests include numerical marine hydrodynamics, ship design optimization and dynamics of offshore structures.